Gas Permeability in Polymer- and Surfactant-Stabilized Bubble Films

Gaëlle Andreatta,[†] Lay-Theng Lee,*[,‡] Fuk Kay Lee,[†] and Jean-Jacques Benattar[†]

Service de Physique de l'Etat Condensé (CNRS URA 2464) and Laboratoire Léon Brillouin (Laboratoire commun CEA-CNRS (UMR 12)), CEA-Saclay, F-91191 Gif-sur-Yvette Cedex, France

Received: June 9, 2006; In Final Form: August 8, 2006

The gas permeabilities of thin liquid films stabilized by poly(*N*-isopropylacrylamide) (PNIPAM) and PNIPAM−SDS (sodium dodecyl sulfate) mixtures are studied using the "diminishing bubble" method. The method consists of forming a microbubble on the surface of the polymer solution and measuring the shrinking rates of the bubble and the bubble film as the gas diffuses from the interior to the exterior of the bubble. PNIPAM-stabilized films exhibit variable thicknesses and homogeneities. Interestingly, despite these variable features, the gas permeability of the film is determined principally by the structure of the adsorbed polymer layer that provides an efficient gas barrier with a value of gas permeability coefficient that is comparable to that of an SDS Newton black film. In the presence of SDS, both the film homogeneity and the gas permeability coefficient increase. These changes are related to interactions of PNIPAM with SDS in the solution and at the interface, where coadsorption of the two species forms mixed layers that are stable but that are more porous to gas transfer. The mixed PNIPAM−SDS layers, studied previously for a single water−air interface by neutron reflectivity, are further characterized here in a vertical free-draining film using X-ray reflectivity.

Introduction

The stabilization of an interface by adsorbed polymers is encountered in numerous colloidal systems, for example, in food and in cosmetics. In cases where gas bubbles are introduced, such as in foam food products, the rheological properties and overall texture and structural stability depend on the dispersion of bubbles.[1] A key parameter therefore is the control of the stability of the bubbles to prevent or retard coalescence and Ostwald ripening. In this respect, the study of diffusion of gas through the liquid film separating the two gas phases is relevant. In this work, we adopt the "diminishing bubble method" to evaluate gas permeation through an aqueous film stabilized by adsorbed polymer and surfactant. The method consists of measuring the rates of shrinkage of a gas bubble and of the bubble film produced at the solution−air interface; from these rates, the gas permeability coefficient K is deduced.

The polymer used in this study is poly(*N*-isopropylacrylamide) (PNIPAM), a thermosensitive nonionic polymer that has a lower critical solubility temperature around 32 °C; above this critical temperature, it dehydrates and phase-separates out of water. In the presence of an anionic surfactant, sodium dodecyl sulfate (SDS), PNIPAM interacts with the surfactant, resulting in resolubilization of the polymer and, hence, an elevation of the lower critical solubility temperature.[2] Results of neutron scattering studies attribute this resolubilization to formation of polymer chains decorated with charged micellar aggregates.[3] Formation of such polymer−surfactant chains is a cooperative process that takes place above a critical surfactant concentration, called the critical aggregation concentration (cac). For the PNIPAM−SDS system, the cac has been determined to be about an order of magnitude below the critical micelle concentration (cmc).[4]

PNIPAM also adsorbs spontaneously at the water−air interface, lowering the interfacial tension to around 40 mN/m. This adsorption can be modulated by several parameters: by temperature due to its thermosensitive nature, and by addition of SDS, due to strong PNIPAM−SDS interactions in the solution. Detailed studies of the adsorption properties of PNIPAM and the effects of temperature and SDS have been carried out using neutron reflectivity and the results reported elsewhere.[5,6]

The ability of the adsorbed PNIPAM layer to stabilize a liquid film has also been shown in thin-film balance measurements.[7] The horizontal thin films formed by this technique are relatively large, $d \sim 500\ \mu$m but are surprisingly stable over periods exceeding an hour. In this work, we are interested in the gas (air) permeability of PNIPAM-stabilized films using the diminishing bubble method,[8,9] where a microbubble is formed on the surface of the polymer solution. From the rates of shrinkage of the bubble and the bubble film, the gas permeability coefficient is evaluated. The results are explained in terms of the structure of the adsorbed PNIPAM layer. The effects of SDS on the film and gas permeation properties are also studied and the results discussed in relation to polymer−surfactant interactions in bulk and at the interface.

Experimental Section

Materials. Two batches of PNIPAM were purchased from Polymer Source (Canada). As per our request, these polymers were synthesized by free radical polymerization in toluene using azobis(isobutyronitrile) (AIBN) as initiator. Their molecular masses, determined by size exclusion chromatography coupled with low-angle light scattering (by P. Lixon, CEA-Saclay) are 90 and 190 K, with polydispersity indices 3.0 and 2.7, respectively. Sodium dodecyl sulfate (SDS, purity ≥ 99%) and sodium chloride (NaCl, purity ≥ 99.5%) were purchased from Fluka Biochemika and used as received. All the solutions were prepared with ultrapure water (18.2 MΩ, Milli-Q system).

* To whom correspondence should be addressed. E-mail: laythen@dsm-mail.saclay.cea.fr.
[†] CNRS URA 2464, CEA-Saclay.
[‡] Laboratoire commun CEA-CNRS (UMR 12), CEA-Saclay.

10.1021/jp063604j CCC: $33.50
Published on Web 09/12/2006

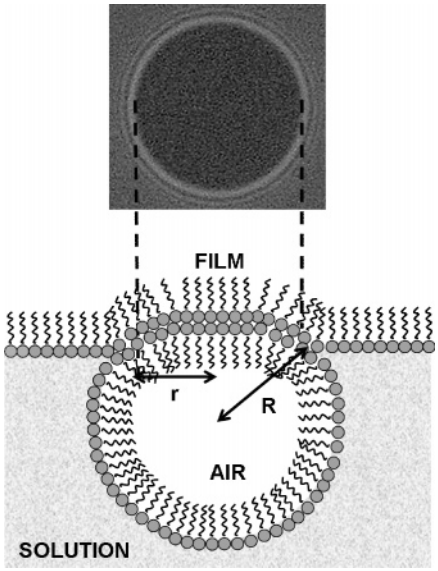

Figure 1. Schematic drawing of a bubble on the solution surface. The top image shows the bubble film that is observed through a microscope; R and r are the radii of the bubble and the film, respectively. The diameter of the film in this case is about 50 μm.

"Diminishing Bubble" Method. The gas permeability coefficient, K (cm/s), across a bubble film is derived as the following,[10] beginning with the gas diffusion equation:

$$\frac{dN}{dt} = -KA\Delta C_g \tag{1}$$

where N is the molar number of gas that permeates the film at time t and A is the area of the film. ΔC_g is the difference in gas concentration at both sides of the film and is expressed as

$$\Delta C_g = \frac{2\sigma}{R}\frac{1}{R_{gc}T} \tag{2}$$

where σ is the solution surface tension, R the bubble radius, R_{gc} the universal gas constant, and T the temperature. Considering the air inside the bubble as an ideal gas:

$$N(t) = \frac{\left(P_{atm} + \frac{2\sigma}{R}\right)\frac{4}{3}\pi R^3}{R_{gc}T} \tag{3}$$

From eqs 1−3, the gas permeability coefficient across the bubble film is derived as[10]

$$K = \frac{\frac{P_{atm}}{2\sigma}(R_0{}^4 - R_t{}^4) + \frac{8}{9}(R_0{}^3 - R_t{}^3)}{\int_0^t r^2\,dt} \tag{4}$$

R_0 is the initial bubble radius at $t = 0$, R_t the bubble radius at time t, and P_{atm} the atmospheric pressure.

Experimentally, a bubble of radius R is blown onto the surface of the solution using a fine capillary tube. The pressure difference (equal to the capillary pressure $2\sigma/R$) between both sides of the film causes gas diffusion through the film from the bubble interior to the outside air (Figure 1). A cap is placed over the cell containing the solution to reduce evaporation. The temperature is kept constant by a thermostat device and by monitoring with a sensitive digital thermometer with an accuracy of ±0.1 °C. The evolution of the bubble radius (R) and the film radius (r) is monitored as a function of time using a microscope connected to a CCD camera and software for image processing. Each reported K value is an arithmetic average of at least five measurements calculated using surface tension values measured separately and published elsewhere.[6] In this study, R_0 ranges from 50 to 250 μm.

Note that eq 4 considers only diffusion of the air across the thin bubble film. A second possible mechanism for the diminishing bubble size is diffusion of air from the bubble into the bulk solution. This process depends on the solubility coefficients of air in the solution at corresponding pressures, P_{atm} and $P_{atm} + 2\sigma/R$. The gas permeability coefficient across the bubble−solution interface stabilized by a monolayer of polymer is thus given by[11]

$$K_b = \frac{P_{atm}}{R_{gc}TS_{atm}t}\left(\frac{P_{atm}}{4\sigma}(R_0{}^2 - R_t{}^2) + \frac{2}{3}(R_0 - R_t)\right) \tag{5}$$

where S_{atm} is the solubility coefficient of air at atmospheric pressure. Experimentally, K_b is measured by placing a clean glass slide over the bubble. Under this condition, air escapes only from the bubble to the bulk solution, thus allowing the determination of the effect of gas solubility on the diminishing bubble size.

X-ray Reflectivity. Vertical films formed from the polymer and surfactant solutions are also studied. The structures and thicknesses of these free-draining films can be determined accurately by X-ray reflectivity measurements.[12,13] The high electron density gradient at the two air−film interfaces, and the constructive interference at these interfaces give rise to strong "Kiessig fringes" that allow the overall film thickness to be determined with high accuracy (±0.5 Å in the present case). The film is drawn from the solution using a rectangular steel frame (35 × 3 mm) and allowed to drain for several minutes. All the experiments are carried out in a sealed box in order to maintain a saturated vapor atmosphere. At the last stage of drainage, the film thickness is small compared to the wavelengths of visible light and the reflected beams at both sides of the film interfere destructively. Under these conditions, the film is black for visible light but allows constructive interference for X-rays. Reflectivity experiments are performed using a copper tube X-ray source (λ = 1.5405 Å, Cu Kα_1 line) and a high-resolution diffractometer (Optix-Nonius) described in detail elsewhere.[13] Reflectivity is defined as $R(q) = I(q)/I_0$, where $I(q)$ and I_0 are intensities of the reflected and the incident beam, respectively, and $\mathbf{q}$ is the scattering wave vector, $q_z = 4\pi(\sin\theta)/\lambda$. The reflectivity profile provides access to the refractive index normal to the film that is related to the reduced electron density, $\delta(z)$, by $n(z) = 1 - \delta(z) - i\beta(z)$, where $\beta(z)$ is proportional to the linear absorption coefficient. In fitting the reflectivity curve, the film is divided into a series of homogeneous slabs and, for each slab, fitted for thickness, reduced electron density, and interfacial roughness using an optical formalism taking into account multiple reflections.[14] The reduced electron density δ of a material is given by

$$\delta = \frac{\lambda^2 r_e}{2\pi}\rho, \quad \text{where } \rho = Z\frac{N_A d}{M_w} \tag{6}$$

where ρ is the mean electron density, Z the atomic number of the element, M_w the molecular weight, N_A the Avogadro's number, d the density of the material, λ the wavelength of the X-ray, and r_e the classical radius of the electron. The goodness of fit is determined by minimization of χ^2.

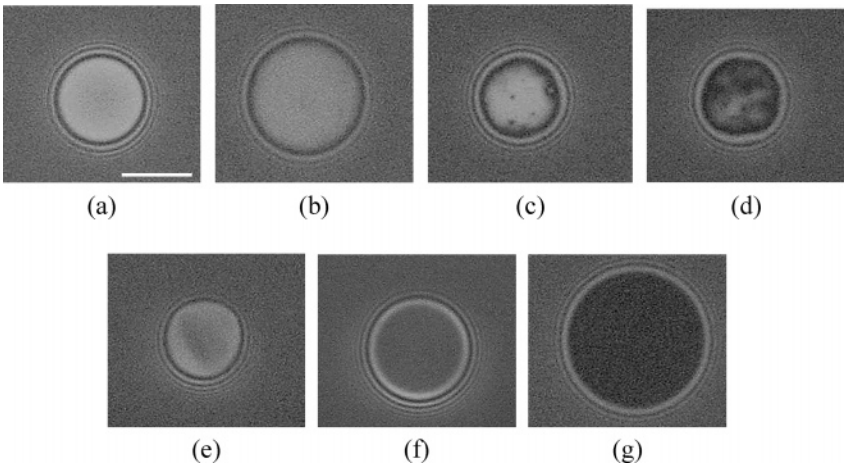

Figure 2. Bright-field optical micrographs of bubble films in the diminishing bubble experiments. Images a−d: Films formed from pure PNIPAM solution. Image e: Film formed from PNIPAM + NaCl. Image f: Mixed PNIPAM−SDS film. Image g: Mixed PNIPAM−SDS film + NaCl. C_p = 1 mg/mL; C_s = 3.46 mM; C_{NaCl} = 0.1 M; $T \approx 22$ °C. (Scale bar = 30 μm.)

Results and Discussions

Gas Permeability of PNIPAM-Stabilized Films. PNIPAM-stabilized air bubbles, ranging from ∼50 to 250 μm in diameter, can be formed on the surface of an aqueous solution of PNIPAM. These bubbles form less easily than surfactant-stabilized bubbles but, once formed, remain stable over a period of several hours, permitting measurement of the gas permeability coefficient (K) across the bubble film. Since small bubbles decrease very quickly below the resolution of the microscope, only bubbles with initial diameter $2R \approx 150-250$ μm are used for the measurements. The films of these bubbles ($2r \sim 50$ μm) are metastable, and measurement of diffusion of gas from the interior to the exterior of the bubble can be made over a period up to about 2 h. Beyond these times, the bubble often remains stable but the size falls below the resolution of the microscope.

The physical appearance of the PNIPAM-stabilized films varies in thickness and homogeneity. Below T = 25 °C, the film is generally homogeneous with uniform color, although different films show variable thicknesses:[15] silver-white ($h \sim$ 700 Å), silver ($h \sim 400-700$ Å), dark gray ($h \sim 300$ Å), and black ($h < 200$ Å). Occasional inhomogeneous films are also obtained; these films have nonuniform color showing a large variation in thickness within the film. Figure 2 shows films formed from PNIPAM solution at C_p = 1 mg/mL at $T \approx 22$ °C (good-solvent condition). Images a and b show homogeneous films with different colors (thicknesses), while images c and d show inhomogeneous films with noncircular borders. The color of these films varies from silver-white ($h \sim 700$ Å) to gray ($h \sim 400$ Å). These variations in film thickness and morphology do not depend on the initial size of the bubble; furthermore, they do not change significantly over the time of measurement (30 min to 2 h). The addition of up to 0.2 M NaCl does not produce a significant change in the film characteristics. Such inhomogeneous films have also been observed in protein systems.[16]

Apart from the variable physical appearance of the film, a second notable observation is its surprisingly large thickness, $h \sim 700$ Å. This value exceeds twice the average adsorbed polymer layer thickness measured at the water−air interface ($L \sim 100$ Å).[6] Both of these features indicate that the film has not drained to its equilibrium thickness and that steric forces between adsorbed polymer layers are not the predominant stabilizing forces of the bubble film. Rather, the film is trapped in a metastable state, where residual polymers in the film form gellike domains that retard draining and thinning of the film. These polymer-rich domains result from temperature fluctuations in the air above the polymer solution. Due to the thermosensitive nature of PNIPAM, small temperature fluctuations can result in significant changes in adsorption density of the polymer[5] and therefore creating heterogeneous microdomains.

Interestingly, despite the variable thickness and homogeneity of the film, the gas permeability does not appear to be affected: for different bubbles formed from the same solution, as well as those formed from different solutions at the same polymer concentration and temperature, the gas permeability coefficients fall within the same range, with an average value of K = 0.045 cm/s ± 30%. The higher dispersion compared to ±10% for surfactant films and ±20% for protein films[11] can be attributed to the inhomogeneity and metastable state of the film. (Uncertainty in the determination of the contact line of the film, and image resolution give an error of ±5%.) In addition, no difference is obtained for polymers with molecular weights of 90 and 190 kDa.

These results show that the gas permeability coefficient is determined principally by the permeability of the adsorbed polymer layer (at the water−air interface). Polymers trapped inside the film and the thickness of the film do not affect gas transfer from the interior of the bubble to the exterior. This insensitivity to film thickness is in contrast to SDS-stabilized films, where K depends on film thickness: K decreases from ∼0.10 cm/s for common black films ($h \sim 100$ Å) to ∼0.03 cm/s for Newton black films ($h \sim 30$ Å). This thickness dependence is explained by an increased ordering in the surfactant monolayer due to normal interactions of the charged layers.[9,17] The structure of the adsorbed polymer layer differs from that of small molecules. For PNIPAM, the concentration profile is characterized by two principal zones: a monomer-rich proximal zone (next to the air phase) and a solvent-rich central zone. The central zone consists of polymer loops and tails, and the monomer concentration decays rapidly toward the bulk solution; this zone thus extends to the order of the radius of gyration of the polymer.[5] The proximal zone, on the other hand, is of the order of the monomer size (∼3−5 Å) and consists of close-packed monomers with surface concentration $\phi_s \approx 1$, independently of polymer chain length. This proximal zone thus provides an efficient barrier to gas diffusion, as evidenced by the relatively low gas permeability coefficient ($K \approx 0.045$ cm/s) compared to other common black films stabilized by

surfactants[17] and by amphiphilic cyclodextrin ($K \approx 0.10$ cm/s).[18] It also explains the nondependence of K on the polymer molecular weight. Thus, gas barrier provided by the PNIPAM film (at $T \approx 22$ °C) is more comparable to that of Newton black films than of common black films of SDS.[17] However, it is less efficient when compared to protein-stabilized films, where $K \approx 0.01$ cm/s measured for several protein molecules.[11] The apparent high efficiency of protein films as gas diffusion barrier is explained by collapsed protein layers that form a dense and viscoelastic film.

Note that, in the diminishing bubble method, the bubble size may also decrease due to gas diffusion to the bulk solution. To evaluate this effect, the evolution of bubble size is measured by placing a clean glass slide over the bubble, as described in the Experimental Section. In this case, the gas permeates only from the bubble into the bulk solution. For the same polymer solution, this term is measured to be $K_b \approx 0.002$ cm/s, a value that is negligible compared to the permeability across the bubble film to the outside air.

Gas Permeability of PNIPAM-SDS Stabilized Films. For solutions containing mixtures of PNIPAM and SDS, the bubbles are formed more easily. All films are homogeneous and circular, with color that varies from silver-white ($d \sim 700$ Å) to dark gray ($d \sim 300$ Å) with increasing SDS concentration, C_s (see Figure 2). In the presence of 0.1 M NaCl, the films become black and common black films (CBF) are obtained ($d \sim 150$ Å). The gas permeability coefficient of the mixed film is also affected accordingly. Due to the increased homogeneity of the films, the dispersion in the gas permeability results is reduced from ±30% for pure polymer films to ±10% at high SDS concentrations. K depends on surfactant-to-polymer ratio. At constant polymer concentration (C_p) and at low SDS, K is close to that of pure PNIPAM solution: $K \approx 0.05$ cm/s (for $C_s < 1$ mM, films of SDS alone are unstable). As SDS increases, K increases abruptly to $K \approx 0.09$ cm/s and remains constant over a small range of SDS concentration; this is followed by a second increase to reach a second plateau at $K \approx 0.14$ cm/s. Note that this plateau value is higher than that obtained for SDS alone, where $K \approx 0.10$ cm/s. (For these mixed solutions, the permeability due to gas diffusion from the bubble to the bulk solution is $K_b \approx 0.01$ cm/s)

The above changes are related to the interaction of PNIPAM with SDS in solution and the corresponding changes in solubility and adsorption behavior of the polymer. Above a cac, SDS interacts with PNIPAM by cooperative association to form a PNIPAM chain decorated with SDS micelles (at 22 °C, cac ≈ 0.7 mM [4]). This charged PNIPAM-SDS chain exhibits polyelectrolyte behavior, with enhanced solubility and reduced sensitivity to temperature. Inhomogeneity in the film caused by temperature fluctuations is thus reduced. In addition, excess charged polymer−surfactant chain is easily displaced from the interfacial region, preventing entrapment in the bubble film. This is evidenced by the thinner and homogeneous films that are obtained with these solutions.

The evolution of gas permeability of the PNIPAM−SDS stabilized film shows a direct correlation with the composition of the adsorbed layer (Figure 3). The composition of the mixed layer, as a function of SDS concentration, has been studied in detail by neutron reflectivity.[19] Three regions can be distinguished: in region 1 ($C_s <$ cac), SDS adsorption is negligible and the surface layer comprises only PNIPAM; thus, the value of K remains unaffected by the surfactant. In region 2 ($C_s >$ cac), PNIPAM is progressively displaced from the surface due to bulk interactions with SDS; here, it can be seen that K increases to a value close to that of SDS alone. The plateau corresponds to the range of SDS concentrations where the PNIPAM and SDS are coadsorbed. In region 3 ($C_s \geq 5$ mM), the polymer chain approaches saturation with bound micelles, and adsorption of the highly charged PNIPAM−SDS chain is energetically unfavorable and is easily displaced from the surface. This follows an abrupt increase in SDS adsorption. Here, only 5−10% of the originally adsorbed PNIPAM is left at the surface and SDS predominates in the adsorbed layer. Thus, with increasing SDS concentration, the gas permeability coefficient evolves accordingly, increasing from a PNIPAM-stabilized barrier to an SDS-stabilized one.

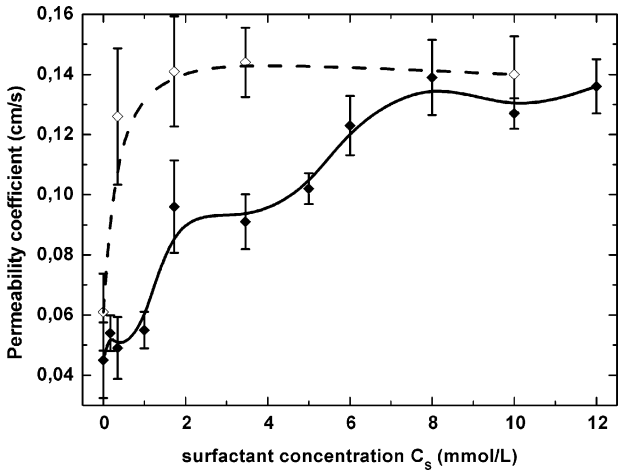

Figure 3. Gas permeability coefficients of PNIPAM-stabilized bubble films as a function of SDS concentration. $C_p = 1$ mg/mL; $T \approx 22$ °C; $C_{NaCl} = 0$ (closed symbols); $C_{NaCl} = 0.1$ M (open symbols). Lines are guides for the eyes.

Note that at high SDS concentration, although the adsorbed layer is SDS-rich, the polymer is not completely displaced from the surface. Rather, the surface consists of a mixed layer of PNIPAM and SDS in equilibrium with the bulk PNIPAM−SDS complex. Interestingly, despite the stability of this mixed layer, as evidenced by its low interfacial tension,[6] the presence of coadsorbed PNIPAM renders the surfactant-rich film more porous to gas permeation compared to a pure SDS layer. This may be attributed to penetration of polymer segment into the surfactant film, as revealed by microcalorimetry studies,[4] that disrupts the lateral interaction and organization of the surfactant molecules. In this region, electrostatic interactions stabilize the film that thins to a common black film ($d \sim 150$ Å) in the presence of 0.1 M NaCl. This thinning in the presence of salt has also been observed in a macroscopic horizontal film measured by thin film balance.[7] The permeability in the presence of 0.1 M NaCl increases more rapidly with SDS and reaches a plateau that joins the curve in the absence of salt. This indicates an earlier onset of displacement of the polymer from the adsorbed layer and that the gas permeability is governed by a surfactant-rich layer. The addition of salt thus induces two effects: enhanced polymer−surfactant interaction resulting in a decrease in cac as reported for other nonionic polymers[20,21] and increased SDS adsorption at the interface due to screening of electrostatic interactions between the surfactant molecules. These two effects contribute to displacement of polymer at lower SDS concentration.

Free Draining Vertical Films. To obtain structural information on polymer- and surfactant-stabilized films, free draining vertical films are studied using X-ray reflectivity. These vertical films have dimensions of about 35 mm in width and 3 mm in height. For pure PNIPAM solutions, the film ruptures before the draining process is completed; this is also the case for pure

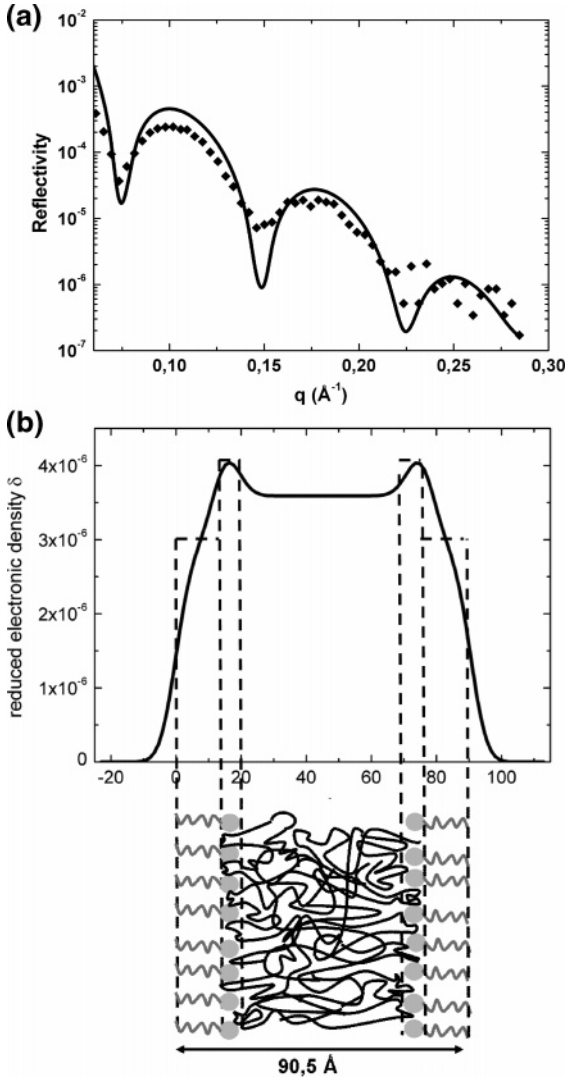

Figure 4. (a) X-ray reflectivity curve of vertical PNIPAM−SDS film. $C_p = 1$ mg/mL; $C_s = 3.46$ mM; $C_{NaCl} = 0.1$ M. The solid line is the best-fit curve using a five-slab model. (b) Fitted electron density profile $\delta(z)$ of the vertical film and schematic diagram showing two outer layers of surfactant hydrophobic tails, two intermediate layers of polar heads, and a central aqueous core containing polymer chains. The total thickness of the film is 90.5 ± 0.5 Å.

SDS solutions in the absence of salt. Therefore under these conditions, metastable films cannot be formed by this method.

For the PNIPAM−SDS mixture at 25 °C, a stable common black film is formed from a solution at $C_p = 1$ mg/mL and $C_s = 3.46$ mM ($C_s >$ cac) in the presence of 0.1 M NaCl. (This point is situated on the plateau region of the gas permeability curve shown in Figure 3.) After about 15 min drainage time, a black film with vertical white lines is obtained. Although these lines indicate nonhomogeneous draining that is linked to the presence of polymer, the film is stable with a lifetime of ∼300 min. Under these conditions, Coulombic repulsion between the SDS-rich monolayers is the stabilizing force in the film.

The X-ray reflectivity curve of the mixed polymer−surfactant black film is shown in Figure 4. Due to the nonplanarity of the free-standing film, the number of counts decreases dramatically, and the quality of the fit could not be improved beyond that shown in the figure. The reflectivity curve nevertheless exhibits three distinct interference fringes that allow determination of the total film thickness with high accuracy, $h = 90.5 \pm 0.5$ Å. Second, a five-layer model is found to give a better fit to the reflectivity profile compared to a three-layer model. The film

TABLE 1: (a) Fitted Parameters for the PNIPAM-SDS Vertical Film Shown in Figure 4

	thickness (Å)	$\delta \times 10^6$
outer layer (hydrophobic tail layer)	12.0 ± 0.1	2.86 ± 0.03
intermediate layer (polar head layer)	6.1 ± 0.1	4.56 ± 0.11
aqueous core (polymer + water)	54.3 ± 0.1	3.59 ± 0.03

(b) Theoretical Reduced Electron Densities of the Different Molecules in the System

	$\delta \times 10^6$		$\delta \times 10^6$
hydrophobic tail of SDS	2.9	PNIPAM	3.79
polar head of SDS	5.2	H_2O	3.56

is thus best described by an aliphatic chain layer, $l_{hc} = 12.0 \pm 0.1$ Å, and an intermediate polar (headgroup) layer, $l_p = 6.1 \pm 0.1$ Å (on each air side) sandwiching an aqueous core, $l_h = 54.3 \pm 0.1$ Å. The fitted parameters are given in Table 1.

The most notable feature of the vertical film formed from the polymer−surfactant solution is the significant increase in total thickness compared to a corresponding SDS common black film in the absence of polymer, where $h_{CBF} = 54.4 \pm 0.5$ Å (at $C_s = 3.46$ mM and $C_{NaCl} = 0.1$ M; at $C_{NaCl} = 0.4$ M, it drains to form a Newton black film, where $h_{NBF} = 32.9 \pm 0.5$ Å [12]). This increase in film thickness arises almost exclusively from the swollen aqueous core (twice that obtained in the absence of polymer) that may be attributed to the presence of polymer and its associated hydration. For the polar layer, a small increase in thickness coupled with a decrease in reduced electron density also suggests the presence of polymer. The aliphatic chain layer remains unmodified by the polymer. These results are consistent with coadsorption of PNIPAM in the SDS layer, as measured by neutron reflectivity[6] and microcalorimetry.[4] Due to the similarity in the electron density values of PNIPAM and water, the fitted electron density of the aqueous core does not provide further information concerning its composition.

From the above results, a free-draining vertical thin film does not appear to bear any direct relation to bubble films in terms of stability and thickness. These differences may be attributed to the film size and the different hydrodynamic process during drainage. For films that are stabilized by PNIPAM alone, the vertical film ruptures before a metastable stage is reached; on the other hand, micrometer-size bubbles that are formed remain stable over several hours. In the case of films stabilized in the presence of SDS, the vertical films are thinner than the bubble films. In this respect, horizontal thin films produced by the thin-film balance method[7] are more closely related to the bubble film. The vertical free-draining film characterized by X-ray reflectivity, however, gives useful information on the composition of the film that complements results obtained at a single water−air interface using neutron reflectivity.[6]

Conclusions

PNIPAM-stabilized bubbles can be formed on the surface on the polymer solution below the critical temperature. The bubble film is metastable and permits measurement of its gas permeability coefficient. Despite the variations in thickness and homogeneity of the film, the gas permeability coefficient across the bubble film is determined principally by the structure of the adsorbed PNIPAM layer. The close-packed proximal region of the concentration profile of the adsorbed polymer layer provides an efficient gas barrier that is comparable to the highly structured SDS Newton black film.

In the presence of SDS, PNIPAM is progressively displaced from the interface due to PNIPAM−SDS interactions in the bulk solution. A mixed PNIPAM−SDS layer, as revealed by

neutron reflectivity at the water−air interface, is also confirmed in a vertical free-draining film by X-ray reflectivity. The gas permeability coefficient in this case is governed by the composition of the adsorbed layer. With increasing surfactant concentration, *K* increases accordingly as the adsorbed layer evolves from PNIPAM-rich to SDS-rich. These mixed polymer−surfactant layers, although stable, show reduced efficiency as a gas barrier compared to those formed by the individual components.

References and Notes

(1) Campbell, G. M., Webb, C., Pandiella, S., Niranjan, K., Eds. *Bubbles in Food*; Eagan Press: St. Paul, MN, 1999.
(2) Schild, H. G.; Tirrell, D. A. *Langmuir* **1991**, *7*, 665.
(3) Lee, L.-T.; Cabane, B. *Macromolecules* **1997**, *30*, 6559.
(4) Loh, W.; Teixeira, L. A. C.; Lee, L.-T. *J. Phys. Chem. B* **2004**, *108*, 3196.
(5) Lee, L.-T.; Jean, B.; Menelle, A. *Langmuir* **1999**, *15*, 3267.
(6) Jean, B.; Lee, L.-T.; Cabane, B. *Langmuir* **1999**, *15*, 7585.
(7) Jean, B. Doctoral Thesis, Université Paris 6, December 2000.
(8) Platikanov, D.; Nedyalkov, M.; Nasteva, V. *J. Colloid Interface Sci*. **1980**, *75*, 260.
(9) Krustev, R.; Platikanov, D.; Nedyalkov, M. *Colloids Surf., A* **1992**, *79*, 129.
(10) Krustev, R.; Platikanov, D.; Nedyalkov, M. *Langmuir* **1996**, *12*, 1688.
(11) Sultanem, C. Doctoral Thesis, Université de Paris XI, December 2004.
(12) Belorgey, O.; Benattar, J.-J. *Phys. Rev. Lett*. **1991**, *66*, 313.
(13) Cuvillier, N.; Millet, F.; Petkova, V.; Benattar, J.-J. *Langmuir* **2000**, *16*, 5029.
(14) Born, F.; Wolf, E. *Principles of Optics*, 6th ed.; Pergamon: London, 1984.
(15) Newton, I.; Opticks, S. S.; Walford, B. London, 1704.
(16) Petkova, V.; Sultanem, C.; Nedyalkov, M.; Benattar, J.-J.; Leser, M. E.; Schmitt, C. *Langmuir* **2003**, *19*, 6942.
(17) Krustev, R.; Platikanov, D.; Nedyalkov, M. *Colloids Surf., A* **1997**, *123*, 383.
(18) Sultanem, C.; Moutard, S.; Benattar, J.-J.; Djedaini-Pilard, F.; Perly, B. *Langmuir* **2004**, *20*, 3311.
(19) Jean, B.; Lee, L.-T. *J. Phys. Chem. B* **2005**, *109*, 5162.
(20) Casford, M. T. L.; Davies, P. B. *Langmuir* **2003**, *19*, 7386.
(21) Bernazzani, L.; Borsacchi, S.; Catalano, D.; Gianni, P.; Mollica, V.; Vitelli, M.; Asaro, F.; Feruglio, L. *J. Phys. Chem. B* **2004**, *108*, 8960.